SPUTTER PROBES AND VAPOR SOURCES FOR ECR ION SOURCES

M. Cavenago*, A. Galatá, M. Sattin, INFN-LNL,Legnaro, Italy
T.Kulevoy, S.Petrenko, ITEP, 117218 Moscow, Russia and INFN-LNL

Abstract

Sputter probes are a promising method for injecting controlled quantities of metallic elements inside ECRIS, provided that the sputter rate can be controlled, so that high charge states and low sample consumption rate will be attained. Moreover pressure at the probe and inside the source should be different. With a sputter probe distance of 25 mm from ECRIS plasma, a 200 nA current of $^{120}\mathrm{Sn}^{18+}$ was easily obtained. Results (for Ti) of an inductively heated rf oven are also discussed. Improvement of sputter probe concepts and geometry are described.

INTRODUCTION

Electron Cyclotron Resonance (ECR) Ion Sources (ECRIS) [1] are the standard source for many nuclear physics complexes, since they can provide highly charged ions ($i^2 > A$ where i is the charge state and A is the mass number) at reasonable current (ranging from $I_i^A \geq 500$ nA to several tens of μA depending on source magnetic field B) and can be optimized for any A. Since gas feeding pose no particular problem, it is therefore of interest and worthwhile to optimize the feeding of any particular metallic element in ECR plasma. While resistive oven are a common option, rf oven were successfully coupled to ECRIS at LNL, using a 14.4 GHz compact ECRIS of relatively old design. Rf oven development, which continues for refractory elements, and preliminary comparison with sputter probe concept recently investigated is discussed in this article.

Oven vapor has a low thermal speed v_{th} (generally believed to be good for trapping inside ECRIS plasma), which distinguishes ovens from breeder concept and from injection with MEVVAs [2], where we can consider a beam velocity v_i. In detail: $v_{th} = (8T_i/\pi m_i)^{1/2}$ where T_i is the ion temperature and $m_i = m_u A$ the ion mass; so $v_{th} = 540$ m/s for tin with $T_i = 0.14$ eV. Moreover $v_i = (2K_i/m_i)^{1/2}$ where the residual ion kinetic energy is $K_i \cong 10$ eV for breeder and $K_i \cong 60$ eV for MEVVA. Forward sputtered atom energy has a broad distribution, maximum at $K_i \cong 4$ eV. So typical v_i estimate are 2.5, 4.0 and 9.8 km/s respectively for sputter, breeder and MEVVA case. Let us state simple estimates of n_e, T_e and of trapping efficiency, which are only provisional. With n_i the density of ion with charge state i and τ_i their confinement time, assuming neglible diffusion across magnetic field **B** lines, the ion current density extracted is $j_0 = \frac{1}{2}eL_{\mathrm{eff}}\sum_i in_i/\tau_i$, where the effective length is $L_{\mathrm{eff}} = \int \mathrm{d}z B_0/|B(z)|$ with

B_0 the field at extraction and z the source axis. Therefore

$$k_2 = 2I_s/(S_0 e L_{\mathrm{eff}}) = \sum_i in_i/\tau_i \equiv n_e/\langle\tau_i\rangle \quad (1)$$

where S_0 is the extraction area, $I_s = j_0 S_0$ is the source current and $\langle\tau_i\rangle$ is an average of τ_i (actually the last equality in eq 1 can be taken as the definition of $\langle\tau_i\rangle$). With $L_{\mathrm{eff}} = 21$ cm, $S_0 = 0.28$ cm^2 and $I_s = 0.50$ mA, we get $k_2 = 1.06 \times 10^{21}$ m^{-3}Hz . Another equation for n_e is approximately given by well known Golovanivsky diagram and the observed extracted current distribution, from which we infer $k_1 = n_e\langle\tau_i\rangle \geq 10^{15}$ m^{3}s, and moreover $T_e \cong 200$ eV. So $n_e = \sqrt{k_1 k_2} \geq 1.03 \times 10^{18}$m^{-3} and $\langle\tau_i\rangle \geq 0.9(7)$ ms. Since electrons are much faster than ions, and neglecting charge exchange contribution, the ionization frequency $\nu_i^+ = n_e\langle\sigma v\rangle$ does not depend on ion speed, so that the mean flight time before ionization of ion X^{i+} is $t_i^f = 1/\nu_i^+$; from Lotz formula at $T_e = 200$ eV for tin, we have $t_0^f = 4.2$ μs, $t_1^f = 11.6$ μs, $t_2^f = 22.2$ μs. A simple condition for trapping is that the first ionization length L_I be much smaller than ECRIS length $L_1 = 18$ cm. This seems very easily satisfied for sputter ($L_I = t_0^f v_i = 1$ cm) and ovens ($L_I = t_0^f v_{th} < 3$ mm). Anyway, experiments with ovens, where metal deposits for a length $L_X \cong 200$ mm from oven, cast some doubts on this models. More detailed modelling, available for breeders, shows that a first ionization is often not sufficient for trapping.

ECRIS working pressure p_a is typically 100 μPa, which is not adequate for sustained sputter. This motivate us to several differential pumping scheme, so that pressure at sputter probe p_p can be larger. More details on rf oven progress are given in the next section. The last section will present sputter probes, first the tubular design and results obtained, then the Penning probe concept and preliminary results. Benefic effect of tubular sputter probes (and similar bias probes) on gas performance is noted.

OVENS

Recent results of rf oven with copper coil for Sn and Pr were described elsewhere [3]; copper coil limits the sample temperature $T_s \leq 1800$ K, but it allows a better efficiency than the Mo coil, used in refractory rf oven.
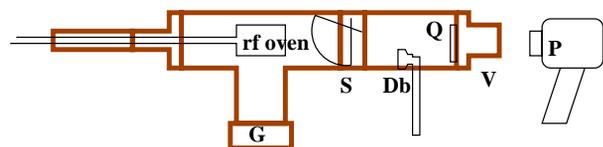
Figure 1: Scheme of oven test facility: vacuum chamber and main parts

Experiments with rf oven for titanium in our ECRIS in 2005 were done with a 140 W rf amplifier A_2, while another amplifier A_3 (350 W nominal) is now available; a new test facility (see fig 1), separated from the ECRIS, was prepared with oven axis mounting horizontal (like in ECRIS). Phenomena which limit oven life into an ECRIS, like bending of crucible and pouring of sample material out of crucible, can be observed and corrected. Crucible bending downwards is due to crucible/stem backlash, and to the limited coupling length $\ell_{cs} \cong 3$ mm; it typically appears after 2 or 3 thermal cycles of oven. Note that Ti reach a large vapor pressure before melting, so that pouring in ECRIS operation is not probable even when crucible is bended (since source operator will adjust heating power to avoid excessive Ti currents). On the contrary, tin pouring can be avoided only with a well aligned crucible, as feasible with a longer $\ell_{cs} \cong 5$ mm coupling.

Test facility is separated by a gate valve G from the main MetAlice vacuum chamber, and can independently vented to air, opened, and be pumped by a rotary pump. In the oven vapor/ligth path we have a shutter S, a slightly off axis deposition balance D_b, a disk of quartz Q where vapor stops, a vacuum viewport V and a pyrometer P. Balance D_b is not affected by the progressive deposit of metal, but it is affected by heat radiated by oven, so that the best measurement protocol is still object of discussion. We now simply leave shutter open in a test procedure, labelled as I. On the contrary metal depositing on Q makes apparent temperature measured by P lower and lower with time; temperature can be reliably measured after cleaning Q and by opening the shutter only when needed (say a total of 400 s in the four hours needed for another oven test, labelled as II). Bias current I_b due a bias voltage V_b applied to crucible is also measured.

Results are given is fig. 2; note that compatibility of tests I and II is good, since oven impedance versus oven power is the same in both cases. Results can be compared to beam produced in the ECRIS source, with power limited to $P_o = 140$ W by amplifier A_2, where extracted beam currents I_i stabilized to modest values for the five ^{48}Ti peaks visible (respectively $I_i = 10, 20, 40, 29$ and 18 nA for $i = 2, 5, 7, 10$ and 11), after some larger values in the initial phase. In both cases, a small crucible bending was visible. Since deposition rate D is about 50 times larger at $P_o = 250$ W than it is at $P_o = 140$ W, a large improvement can be expected for ECRIS currents, at least for lower charge states as Ti^{5+}. By continuing test II over $P_o = 250$ W, we also reach $T_s = 2350$ K, when apparently no Ti was left. Figure 3 shows rf oven mounted in the insert tube which is part of the ECRIS, with well visible evaporation material marks on an iron ring and on this tube. Due to the close proximity between rf coil and crucible, rf voltage makes the bias voltage V_b more negative at low power P_o; on the contrary, at beam production temperature, the current saturates at $I_b \cong -0.6$ mA and V_b drops (in absolute value) to about -200 V, probably due to a conduction in the overheated Mo coil insulating cover. Note that after oven
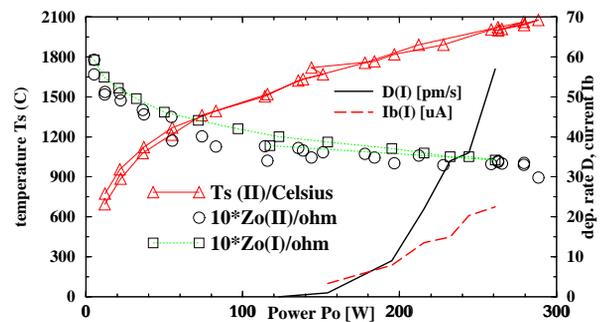
Figure 2: Refractory rf oven results for Ti with procedures I and II; note also I_b the bias current with a $V_b = -20$ V

Figure 3: View (looking from plasma position) of the rf oven. Tube outer diameter 63 mm.

cools, or with oven power off, a voltage V_b up to a few KV can be applied. When oven is not in use, oven crucible acts generally as a bias voltage probe does (that is, a moderately negative V_b improves extracted ion currents).

In conclusion, all principle issue in $T_s > 2200$ K rf oven are solved, and only amplifier problems or crucible/stem coupling or ECRIS schedule delay results. We also noted that Xe current increased after a Pr evaporation, $I_{18}(^{132}\text{Xe}) = 950$ nA instead of 500 nA.

SPUTTER PROBES

Since oven performance improves with a negative sample voltage V_b, we investigate how much beam can be obtained from a probe made of tin (adequately supported) or of Pr, held at a distance L_{oe} outside the ECRIS plasma. In perspective, this has the advantage of simplicity and of avoiding metal melting and perhaps pouring. On the other side, oven vapor production can be simply regulated by increasing P_o.

Design of tubular sputter probe 3 is shown in fig 4: we aligned the ECRIS axis z and the mullite tube, where we constrain the gas feed of the ECRIS to flow. The well-known hollow cathode configuration (should) work to amplify electron emission[4]. This was inspired by previous runs with sputter probes 1 and 2 inclined with respect to z, which show limited bias current $I_b = -0.1$ mA even at $V_b = -5$ kV and negligible yields like $I_{18}(^{120}\text{Sn}) < 50$ nA or similar, both with O or N as buffer gas. Mullite tube also protects the cathode from radial sputtering, and the sputtered atoms exit from the tube if they have a large v_z/v_r velocity ratio. So net sputtering should be directed
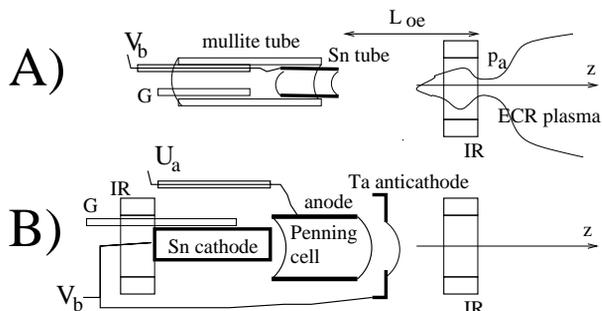
Figure 4: Sputter probe concepts [most isolators and supports not shown; G gas input; IR iron rings]: A) axial hollow tin cathode; B) Penning.

Figure 5: A): spectra of tin/oxygen plasma, with a tin sputter probe and $P_k = 78$ W, $I_s = 450$ μA and $p_g = 340$ μPa; B) tin spectra, with nitrogen, and $P_k = 95$ W

Figure 6: A) Penning current I_a vs pressure p with $p_0 = 10^{-6}$ mbar; B) Penning current I_a vs voltage V_a; comparison with ECRIS experiment

forward.

Using O as a buffer gas, sputter probe 3, mounted axially with $L_{oe} = 22$ mm, produced up to 210 nA of ^{120}Sn^{18+} with $V_b = -3$ kV and $I_b = -0.5$ mA, see fig. 5. With N buffer gas, we get up to 260 nA in the ^{118}Sn^{18+} peak while the larger $A = 120$ peak detection was deformed by nitrogen large peak; this current was obtained by also rising microwave power $P_k = 95$ W. Test lifetime was limited by tin melting.

In the case of Pr, with $L_{oe} = 15$ mm, voltage V_b was limited from the larger I_b emitted, due to well known Pr behaviour with oven. Results up to now was poor, with large uncertainty due to O^{2+} background. Sample was not appreciably consumed by sputtering. Tubular probes act also as bias disks (which refurbish the ECRIS plasma of electrons, so contributing to ionization), and concentrate these electrons on axis, which may be advantageous. Indeed, after completing test for metal production, the same probe was used for a verification of ion source yields with Ne, Ar, Kr and Xe, which were compared to historical best values without vapor sources, using generally the same gas buffer and microwave power P_k. Comparison historical values are $I_4^{22} = 3200$ nA for Ne, $I_{15}^{84} = 690$ nA for Kr (with O buffer) and $I_{18}^{132} = 500$ nA for Xe (with O buffer). To quote a few peak results, with Sn probe we get $I_9^{40} = 4200$ nA for Ar, $I_{15}^{84} = 950$ nA for Kr (with N buffer) and $I_{18}^{132} = 740$ nA for Xe (with O buffer). With Pr probe, we got $I_4^{22} = 4400$ nA for Ne, $I_9^{40} = 8160$ nA for Ar, $I_{15}^{84} = 1210$ nA for Kr and $I_{18}^{132} = 810$ nA for Xe. Results critically depend on gas pressure tuning.

In the design of the Penning probe, we noted that at cathode position $L_{oe} = 58$ mm the fringe magnetic field of ECRIS B_f is about 1. kG and is diverging. We add an iron ring and an iron pole behind the Penning cathode, so that B_f becomes approximately uniform in the whole Penning cell: $B_f = 2.1 \pm 0.1$ kG. In the estimate of Penning current I_a, known from its application as an ion pump[5], an uniform field $B = 2$ kG and nitrogen gas are assumed: $I_a = k_1 p^{1.2} L_a (R_a B)^2$ when $B < B_{tr}$ (low magnetic field mode), where p is gas pressure in mbar and $B_{tr} = k_2 U_a^{1/2}/R_a p^{0.05}$ is a threshold (in Gauss), with U_a the anode voltage, R_a and L_a the Penning cell radius and length in cm, and the constants $k_1 = 0.000293$, $k_2 = 7.52$. In the
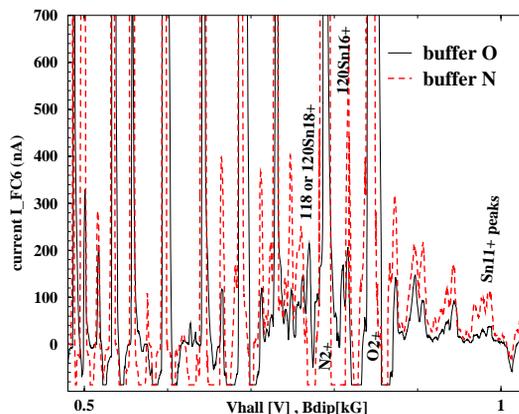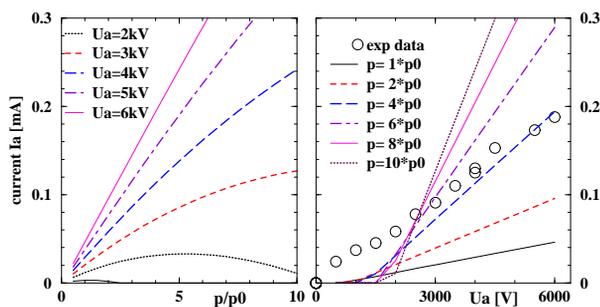
opposite case, $I_a = k_3 p^{1.1} L_a [U_a - k_4 \sqrt{R_a p (B - B_{tr})}]$ with $k_3 = 0.01656$ and $k_4 = 17300$. Result for a few U_a are plotted in fig 6.

Preliminary results of the Penning sputter probe for tin, still in the conditioning phase, show an ECRIS extracted current $I_{18}^{116} \cong 90$ nA and $I_{13}^{120} \cong 160$ nA, with nitrogen gas, with $U_a = 4.2$ kV and $V_b = -80$ V. In this condition, anodic current I_a is modest $I_a = 80$ μA, while cathode current is large $I_b = -300$ μA. By decreasing $|V_b|$, more ECRIS plasma arrives to Penning, so that I_a increases, while I_{18} decreases. Optimization of the system is in progress.

We thank D. Giora for the construction of the new Penning sputter probe.

REFERENCES

[1] R. Geller, *Electron Cyclotron Resonance Ion Sources and ECR Plasmas*, Institute of Physics Publ.,Bristol,1996.

[2] A. V. Vodopyanov et al. , Rev. Sci. Instrum., **75** (2004) 1888

[3] M. Cavenago, A. Galatá, T. Kulevoy, S. Petrenko, Rev. Sci. Instrum., **77** (2006), 03A339

[4] A. T. Forrester, *Large Ion Beams*, John Wiley, NY, 1996

[5] J. Hartwig, J. S. Kouptsidis, J. Vac. Sci. Technol., **11**, (1974) 1154